



Removal of Ag (I) ions using potassium nickel hexacyanoferrate ion exchanger incapsulated barium alginate from aqueous solutions.

Abdel- Fattah Fadel Shaaban, Mohammed Morsy Azab, Asmaa Said*

Chemistry Department, Faculty of Science, Benha, Egypt.

*Corresponding author e-mail: asmaahgazy00@yahoo.com

Abstract

Spherical beads of potassium nickel hexacyanoferrate ion exchanger incapsulated barium alginate (KNiHCF-Ba-alginate) have been prepared by ionotropic gelation of nickel chloride, potassium ferrocyanide with sodium alginate in the presence of BaCl₂ solution. The composition, properties and morphology of the resulting ion exchanger have been characterized by Fourier transform infrared (FTIR) spectroscopy, scanning electron microscopy (SEM), x-ray diffraction (XRD) and thermogravimetric analysis (TGA). Batch technique was employed to examine the effects of different parameters such as solution pH, concentration of metal ions, contact time and medium temperature on silver ion uptake. The results indicated that the barium–alginate ion exchanger have high affinity towards silver ions. The ion exchange data have been perfectly described by Freundlich isotherm rather than other isotherms such as Langmuir and Temkin. Kinetics data have been analyzed using pseudo-first order, pseudo-second order and intra-particle diffusion equations. The resulted showed that pseudo-second-order kinetic model was best fit with the obtained data. Also, thermodynamic data proved the spontaneity of sorption process. Furthermore, the removal of silver ions using KNiHCF-Ba-alginate has been studied using column technique as well.

Keywords: Potassium nickel hexacyanoferrate, ion exchanger, barium alginate, morphology, isotherms, kinetics, thermodynamics.

Received; 21 July 2018, Revised form; 12 Sept. 2018, Accepted; 12 Sept. 2018, Available online 1 Oct. 2018

1. Introduction

The study of heavy metal removal from drinking water and industrial wastewater gained lately strong concern since they accumulated in living organism and cannot be biodegraded, thus causing several diseases when exceed specific limits [1,2]. High concentrations of the metals in solution affect humans, animals and vegetation. The pollution of water and soil with metal cations increases proportionally with the expansion of industrial activities [3, 4]. In order to minimize processing costs for these industrial wastewaters, most of the last investigations have focused on the use of low cost adsorbents [5-7].

Silver is a very useful raw material in various industries due to its excellent malleability, ductility, electrical and thermal conductivity, photosensitivity and antimicrobial properties. Significant amounts of silver are lost in the effluents discharged from such industries and due to the toxicity of silver to living organisms, the removal of this metal from wastewaters is an important concern.

The presently available technologies for the removal of silver include precipitation, electrolysis, solvent extraction, use of ion-exchange resins, chelating agents, etc. These processes can be profitably used on a large scale when the metal concentrations in effluents are sufficiently high, i.e., above 0.93mmol/L [8,9]. However, most of these processes are unacceptable, owing to the

disposal of sludge their high cost, low efficiency and inapplicability to a wide range of pollutants [10].

Following methods have been used by researchers for removal of heavy metals. Physical separation techniques are primarily applicable to particulate forms of metals, discrete particles or metal bearing particles [11]. Recently, Khan et al. studied the adsorption of silver on bentonite by a batch technique. Distribution coefficients were determined for sorption systems as a function of contact time, pH, sorbent and sorbate concentration and temperature [12].

Hanzlǐk1 et al studied twelve carbonaceous materials that were investigated for adsorption of Cd, Cu and Ag from water. The batch adsorption experiment was used. The kinetic of the adsorption process was very fast for the first five hours but very slow for approximately the next 65 hours [13]. Hsuan et al studied the adsorption capacity of eggs hells with membrane (ESWM), eggshell membrane (ESM), and eggshells (ES) for the removal of nickel and silver ions in synthetic wastewater. The 0.8 g of ESM could remove 90.91 % of nickel ions (100 mg/L) at 25 °C, pH 5.76 and 24 h. On the other hand, approximately 100 % of silver ions (25 mg/L) could be removed by 0.2 g of ESM at 25 °C, pH 5.2, and 24 h [14].

Rakchaiyawan et al studied chitosan-polyvinyl alcohol resin as adsorbent of silver ion. Batch kinetic experiments were carried out. The adsorption capacity of blend chitosan-polyvinyl alcohol resin at 0.5 g and 100 mg/L was 19.1 mg/g. It was found that the pseudo-second order model was fit for describing the adsorption behavior [15].

Lawler et al investigated whether such particles could be expected to be removed in conventional water treatment plants such as flocculation and filtration. Both flocculation and granular media filtration experiments with citrate-capped silver nanoparticles were performed at different ionic strengths and in the presence and absence of natural organic matter. The results were generally consistent with theories of particle destabilization that have been developed for larger particles (greater than 1 μm), suggesting that silver nanoparticles are likely to be removed in conventional treatment processes [16].

Gedanken et al disclosed a new approach for the removal of heavy metal ions from water, using a combined procedure composed of two technologies, namely, spontaneous adsorption of heavy metal ions on aquatic plants and conversion of the adsorbed heavy metal ions into the corresponding metallic nanoparticles by the polyol reaction carried out in a microwave oven. For removing silver in this research, they studied the complete spontaneous adsorption of Ag^+ ions on the aquatic plants *A zolla? liculoides* took a few days (about 7 days). Reduction of the adsorbed heavy metal ions to the metallic nanoparticles was carried out by microwave irradiation for 3 minutes of an ethylene glycol solution of the Ag^+ -adsorbed plant biomass [17].

In the present work spherical beads of (KNiHCF)-Ba-alginate have been prepared by ionotropic gelation of nickel chloride, potassium ferrocyanide with sodium alginate in the presence of BaCl_2 . The factors affecting the removal behavior of silver ions such as pH of the solution (0.5-7.0), metal ion concentration, contact time and temperature were investigated using batch method. The obtained equilibrium data were analyzed using three models: Langmuir, Freundlich and Temkin. Kinetic and thermodynamic parameters, of Ag^+ ions exchange, were also calculated. Moreover, fixed bed column method was used for the adsorption of silver ions.

2. Materials and Methods

2.1. Materials

Silver (I) nitrate (AgNO_3) was used in the adsorption experiments purchased from Sigma-Aldrich Co., USA. pH adjustments were carried on using 0.1 N Nitric acid (HNO_3) and 0.1 N sodium hydroxide (NaOH). All Ag^+ solutions were prepared with ultra-pure water (specific resistivity of 18 MW. Cm) obtained from an E-pure (Barnstead, USA) purifier system. Super purity nitric acid (SpA, 68 %) purchased from Sigma-Aldrich Co., USA. Potassium ferrocyanide (KFC), nickel chloride ($\text{NiCl}_2 \cdot 6\text{H}_2\text{O}$), sodium alginates were pure grade products of Merck Co., Germany and were used directly. Barium chloride was purchased from Sigma-Aldrich Co., USA.

2.2. Synthesis

2.2.1. Preparation of potassium nickel hexacyanoferrate

Solution of potassium ferrocyanide (KFC) (167 ml, 0.1 M) was dropping on solution of NiCl_2 (500 ml, 0.1 M) slowly at room temperature with vigorous stirring then heating to 80 °C in water bath for 4 hours, then stop heating and stirring and leave it to 24 hours to make coagulation. Washing the precipitate about 8 times with total volume two liters of water then centrifuge the precipitate and dry it until give constant weight then ground the precipitate.

2.2.2. Preparation of (KNiHCF)-Ba-alginate

Added sodium alginate (2.4 g) on potassium nickel hexacyanoferrate solution slowly with strong stirring for 3 hours to form suspension solution of gelatin media. This solution was dropping into solution of BaCl_2 (9.7 g, 0.2 M) dissolved in 200 ml distilled water using syringe with suitable needle 18G making slow flowing with slowly stirring. Leave the beads on stirring for 3 hours then leave it for 3 days. Then, the beads were separated from the solution and washed with water several times and drying.

2.3. Instrumentation

2.3.1. Scanning electron microscope (SEM)

Scanning electron microscope was used to observe the surface morphology and particle size of the ion exchanger resin synthesized. Micrographs were obtained using (QUANTA 250 SEG, HOLANDA) micro analyzer microscope. The samples were prepared by deposition of a thin gold film, sputtered using a Balzer SCD 050 deposition system.

2.3.2. FT-IR measurements

The IR spectrum of the ion exchanger was measured as KBr pellets using FT/IR-BRUKER, Vector 22(Germany) Spectrophotometer.

2.3.3. Thermal gravimetric analysis (TGA)

Thermal analysis experiments including thermal gravimetric analysis (TGA) and differential scanning calorimetry (DSC) for the ion exchanger were carried out using SDT Q600 V20.5 Build 15 Thermo gravimetric analyzer. The experiment was performed in a dynamic atmosphere of nitrogen from room temperature to 1000 °C at heating rate of 10 °C/min.

2.3.4. X-ray diffraction (XRD)

The X-ray diffraction of ion exchanger in powder form was obtained from Diano X-ray diffractometer using $\text{Cu K}\alpha$ radiation ($\lambda = 1.5418 \text{ \AA}$). The scanning range was between angle $2\theta = 0$ to 60 for ion exchanger.

2.3.5. Determination of the metal ions concentration

Metal ions concentration was determined by using Hitachi atomic absorption Z-6100 polarized Zeeman spectrometer.

2.4. Adsorption of metal ions

2.4.1. Uptake of metal ions using batch method

All experiments were performed with 0.1 g resin in 250 ml bottles with 100 ml of single metal ion solution on a temperature-controlled shaker at 200 rpm. All experiments were carried out at 25 °C except the temperature experiments. The desired pH of solution was adjusted using few drops of 0.1 M HNO_3 and 0.1 M NaOH solutions. Concentration of the metal ions in the solution was determined by titration (Volhard's Method).

Experiments were carried out in triplicate. The adsorption capacity was calculated according to Eq.1.

$$Q_e = \frac{C_o - C_e}{W} \times V \tag{1}$$

where Q_e is the adsorption capacity (mmol/g). C_o and C_e are the initial and the equilibrium concentrations of metal ions (mmol/L), respectively. V is the volume of metal ions solution (L) and W is the weight of dry resin (g). Determination of the optimum pH for adsorption of metal ions, were carried out by shaking 0.1 g of resin with 100 ml (2.3mmol/L) metal ion solution for 3 hrs at adjusted pH. Experiments of adsorption isotherms were performed by shaking 0.1 g of resin with 100 ml of metal ion solution at optimum pH in a concentration ranging from 1.85 to 8.33 (mmol/L). After 3 hrs of shaking, the resin was filtered and the remaining metal ion concentration in solution was estimated. To investigate the adsorption kinetic of the adsorption process, 0.1 g of resin and 100 ml of metal ion solution was continuously shaken at optimum pH and concentration at 25 °C. The flasks containing the mixtures were withdrawn at different time intervals to determine the remaining concentration of metal ions. Measurement of metal ion adsorption by the resin as a function of temperature was studied in the temperature range of 35–55 °C. Experiments were performed by shaking 0.1 g of resin with 100 ml of metal ion solutions (2.3 mmol/L) under the optimum pH and contact time. After adsorption, the residual concentration of metal ion was determined as described earlier.

2. 4. 2. Uptake of metal ions using column technique

A continuous adsorption experiment was carried out in laboratory-scale glass column (20 cm height and 1.2 cm diameter) filled with(KNiHCF)-Ba-alginate resin, forming a homogeneous and well-packed bed. The performance of fixed-bed column was described through a break-through curve and expressed as the ratio of effluent metal ion concentration over influent metal ion concentration (C_{eff}/C_o) as a function of time (t). For optimizing the column dynamic, adsorption experiments were carried out at different bed heights (9, 18 cm), two constant flow rates (1, 2, 3 ml/min), 0.41mmol/L single metal ion concentration and optimum pH at 25 °C. First of all, the column was cleaned by enough rinse the adsorbent. The performance of the column adsorption processes is based on the breakthrough curve which is obtained by plotting C_{eff}/C_o Vs time (t), where C_{eff} and C_o are effluent and influent metal ion concentration (mmol/L), respectively. The mass transfer zone (Δt) [18] is given by Eq. 2.

$$\Delta t = t_e - t_b \tag{2}$$

where t_b is the break-through time (which is the time needed for the increase of metal ion concentration in the effluent to an appreciable value in a sudden way) and t_e is the bed exhaustion time (which is the time needed for the increase of metal ion concentration in the effluent exceeding 99 % of the influent concentration). The length of the mass transfer zone (Z_m) [18] is obtained from the break-through curve and is calculated from Eq. 3.

$$Z_m = Z \left(1 - \frac{t_b}{t_e} \right) \tag{3}$$

where Z is the bed height in mm. The total column adsorption capacity (q_{total}) [19] is calculated from Eq. 4.

$$q_{total} = QA/1000 = Q/1000 \int_{t=0}^{t_{total}} (C_{ad})dt \tag{4}$$

where A is the area under the break-through curve of the plot between C_{ad} ($C_{ad} = C_o - C_{eff}$) versus time, Q is the flow rate (ml/min) and

t_{total} is the total flow time (min). The equilibrium adsorption capacity ($q_{eq (exp)}$) (mmol/g) [18] is calculated by Eq. 5.

$$Q_{eq (exp)} = \frac{q_{total}}{m} \tag{5}$$

where m is the total dry weight of (KNiHCF)-Ba-alginate resin (g). The total amount of metal ions fed to the column is calculated from Eq. 6 [18].

$$W_{total} = \frac{C_o Q t_{total}}{1000} \tag{6}$$

where W_{total} is the whole amount of metal ion placed inside the column. Total percentage removal of metal ions (%) is calculated from Eq. 7 [18].

$$(\%) = \frac{q_{total}}{w_{total}} \times 100 \tag{7}$$

3. Result and discussion

3. 1. Characterization of (KNiHCF)-Ba-alginate

3. 1. 1. FT-IR spectra

Fig. 1 showed IR spectrum of the synthesized potassium nickel hexacyanoferrate (KNiHCF)-Ba-alginate beads, which showed characteristic peak at 3380 cm^{-1} attributed to OH stretching, band at 1597 cm^{-1} for COOH stretching, 1031 cm^{-1} corresponding for C-O-C stretching and sharp peak at 2090 cm^{-1} related to $C \equiv N$ stretching.

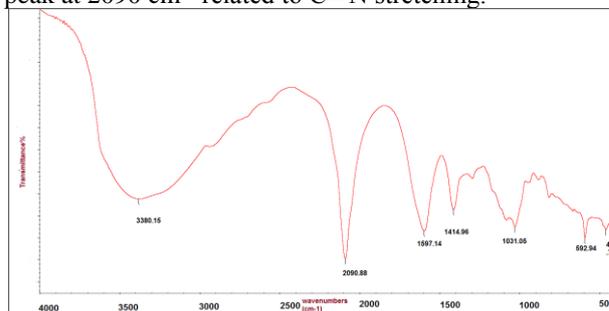


Fig (1): FT-IR spectrum of the synthesized potassium nickel hexacyanoferrate (KNiHCF)-Ba-alginate beads.

3. 1. 2. Thermal gravimetric analysis (TGA)

The thermal stability of the beads and their water content were determined by thermogravimetric. A known amount of the surface-dried swollen beads was heated in an alumina crucible at a heating rate of 10 °C min^{-1} under nitrogen atmosphere. TGA of the beads was shown in Fig. 2. In the TGA weight loss is observed at 31 °C, which continues up to 163 °C, with a total weight loss of ~6.3 %, due to the loss of the absorbed water molecules. Then, the second degradation step was observed from 226 to 544 °C, with a total weight loss of ~28.7, which due to the evolution of CO_2 . The third stage was observed from 600 to 896 °C, which represents degradation of skeletal alginate chain structure. At the end of 896 °C the mass was left as a residue.

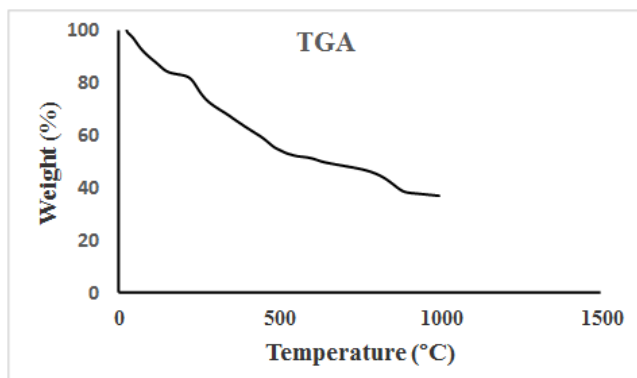


Fig (2): TGA of the synthesized (KNiHCF)-Ba-alginate beads.

3.1.3. X-Ray diffraction

Fig. 3. showed the X-ray powder diffraction pattern of the synthesized KNiHCF-Ba-alginate beads was recorded using CuK α radiation. The diffraction pattern obtained had broad diffraction peaks, indicating the crystalline nature of the KNiHCF particles. The main diffraction peaks were observed at 2θ values of 17.56° , 25.05° and 35.49° , which match well with those reported for $K_2Ni[Fe(CN)_6]$ (JCPDS card no. 20-0915). Thus, the results of the XRD study confirmed the presence of crystalline KNiHCF in the synthesized beads.

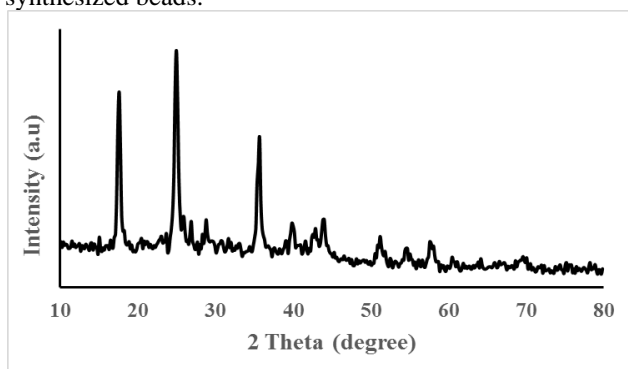
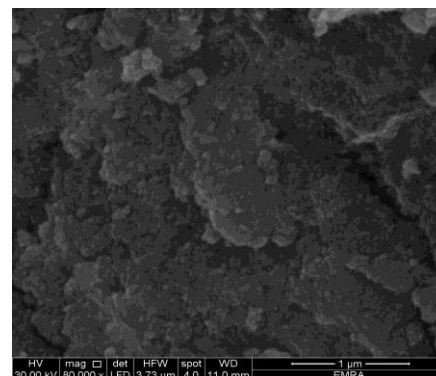


Fig (3): X-ray diffraction of the synthesized (KNiHCF)-Ba-alginate beads.

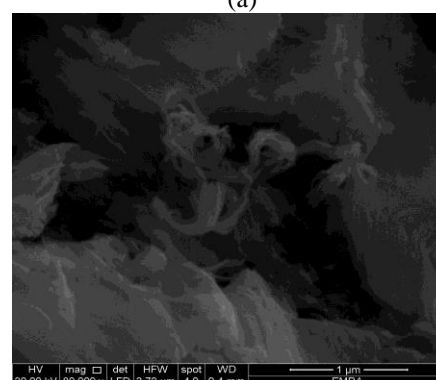
3.1.4. Scanning electron microscope (SEM)–EDX

The surface morphology of the resin was examined by scanning electron microscopy and energy dispersive x-ray microanalysis (EDX) system. The scanning electron micrograph images of the synthesized (KNiHCF)-Ba-alginate beads and beads captures Ag^+ ions were shown in Fig. 4(a) and (b), respectively. The morphology of (KNiHCF)-Ba-alginate beads before metal ion uptake showed thick surface. After metal ion uptake, the beads surface became totally covered by silver ions adsorption. The presence of silver ions in the synthesized (KNiHCF)-Ba-alginate beads was confirmed from energy dispersive x-ray spectroscopy (EDX) measurements (Fig.5(b)). The resin with Ag^+ ions showed distinct signals at 2.7, 3.0, 3.2 and 3.5 keV. The objective of this analysis was to map elemental Ag^+ ions qualitatively (not quantitatively) on the composite surface. However, the level of the Ag signal

observed was sufficient for providing a qualitative idea of the homogeneous distribution of Ag element at the surface of the sorbent: the percentage (in mass) of Ag was 62.68 %.



(a)



(b)

Fig (4): Scanning electron microscope (a) (KNiHCF)-Ba-alginate beads (b) (KNiHCF)-Ba-alginate beads with Ag^+ ions.

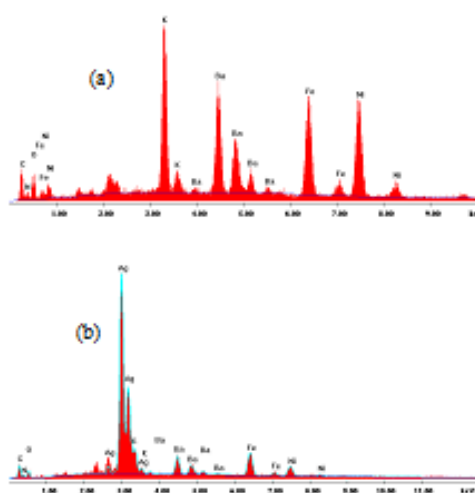


Fig (5): EDX, (a) (KNiHCF)-Ba-alginate beads (b) (KNiHCF)-Ba-alginate beads with Ag^+ ions.

3. 2. Uptake of metal ions by batch technique

3. 2. 1. Optimum pH of metal ions uptake

The influence of the pH on the uptake capacity of metal ion was examined by batch system at $25^\circ C$ in the pH range of 0.5–7.0 and the results were presented in Fig. 6.

The results showed that the capacity increased when the pH value was increased until it reached to the maximum (optimum value). The optimum pH value which resulted in the greatest adsorption capacity for metal was located at 7.0. For this work all the consequent experiments were performed at optimum pH. Above optimum pH, metal was converted to precipitated metal chloride and the adsorption of these ions cannot be measured accurately.

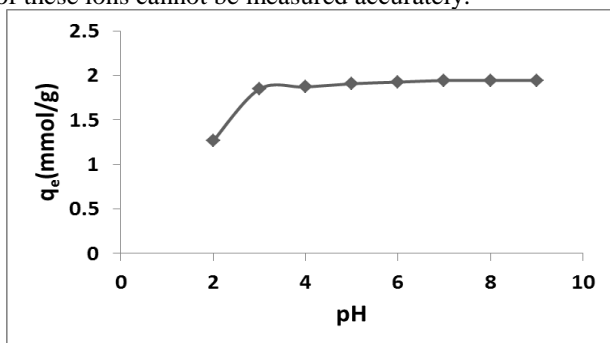


Fig (6): Effect of pH on the amount of sorbent of Ag⁺ ions on (KNiHCF)-Ba-alginate at 25 °C and shaking time 3hrs.

3. 2. 2. Effect of initial concentration of Ag⁺ ions

The influence of the initial metal ion concentrations on equilibrium adsorption was performed at initial concentrations of 1.85, 3.7, 5.56, 6.48, 7.41 and 8.33 mmol/L at 25 °C, shaking time 3 hrs and pH 7 for the sorption of Ag⁺ ions on (KNiHCF)-Ba-alginate and the results were illustrated in Fig.7. The results showed that the amount of Ag⁺ onto (KNiHCF)-Ba-alginate increased as the initial concentration of metal adsorbed ions increased before reaching a plateau shape. The maximum adsorption capacity was obtained at optimum pH and at 25 °C was illustrated in Table 1. The results showed that the maximum adsorption capacity of Ba-alginate resin reached to 3.9 mmol/g at maximum initial concentration of 7.4 mmol/L.

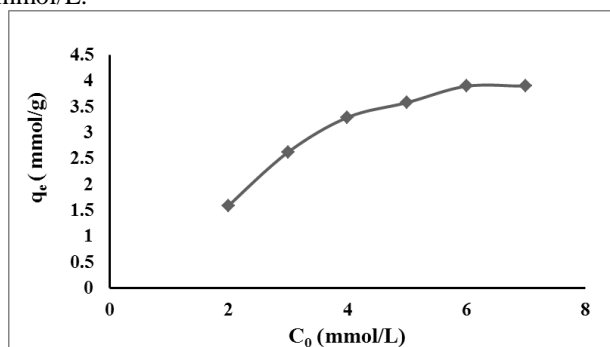


Fig (7): The Effect of initial concentration of Ag⁺ ions on (KNiHCF)- Ba-alginate at 25 °C, shaking time 3hrs and pH 7.

Equilibrium isotherm data were analyzed using Langmuir, Freundlich, and Temkin isotherm models. The Langmuir isotherm model is based on the adsorption of the mono layer of metal ions onto a homogenous surface of the chelating resin. The linear form of Langmuir adsorption model is represented as [19].

$$\frac{c_e}{q} = \frac{c_e}{Q_{max}} + \frac{1}{K Q_{max}} \quad (8)$$

where C_e is the equilibrium concentration of metal ions (mmol/L), q is the equilibrium adsorption capacity (mmol/g), Q_{max} (mmol/g) and K (L/mmol) are the maximum adsorption capacity and binding constant, respectively. With the slope and intercept of the linearized plot of C_e/q_e versus C_e (Fig. 8) the parameters of Langmuir model were calculated and listed in Table 1.

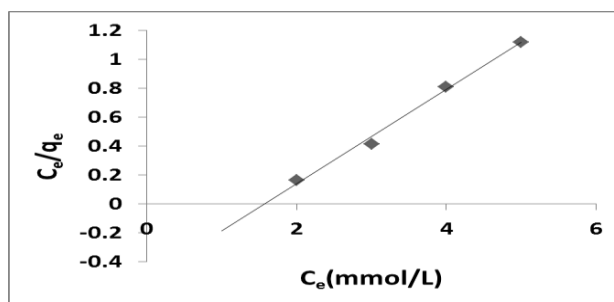


Fig (8): Langmuir adsorption isotherm of Ag⁺ ions on (KNiHCF)-Ba-alginate at 25 °C.

Langmuir isotherm model also defined in terms of the dimensionless parameter known as separation factor (R_L) [20] which is represented as follows:

$$R_L = \frac{1}{1 + K C_o} \quad (9)$$

where K is the Langmuir constant (binding constant) and C_o is the initial concentration of metal ion (mmol/L). The value of R_L which was calculated recommends the shape of the isotherm to be unfavorable (R_L > 1), linear (R_L = 1), favorable (0 < R_L < 1), or irreversible (R_L = 0) [21,22]. Plotting R_L versus C_o was shown in Fig. 9. The calculated values of R_L were between zero and one for metal ions revealed that the metal ion adsorption onto on Ba-alginate resin was favorable. As indicated in Fig. 9, the R_L values decreased as the (C_o) of metal ions increased which showed that the adsorption of metal ions was more effective at higher initial concentration.

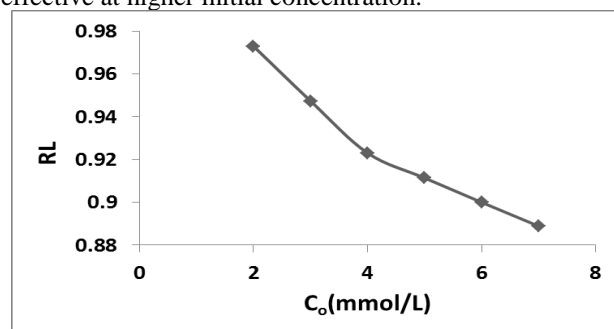


Fig (9): Variation of adsorption intensity (R_L) with initial metal ion concentration (C_o).

The Freundlich isotherm model is an empirical equation which refers to heterogeneous adsorption system. The Freundlich isotherm model was shown by the following equation [23]:

$$\text{Log}q_e = N \text{log}C_e + \text{log}K_F \quad (10)$$

where q_e is the equilibrium adsorption capacity (mmol/g), C_e is the equilibrium concentration of metal ion (mmol/L), K_F and N are the Freundlich constants for the adsorption capacity (mmol/L) and a measurement of efficiency of adsorption, respectively. When $\log q_e$ was plotted against $\log C_e$, a straight line with slope N and intercept $\log K_F$ was obtained (Fig. 10). The values of K_F & N were calculated and collected in Table 1. The value of term N in the Freundlich isotherm model presented the nature of isotherm to be unfavorable ($N > 1$), favorable ($0 < N < 1$) or irreversible ($N=0$). The values calculated for N ranges between (0) and (1) for all metal ions which refers to the simplicity of adsorption process of metal ions onto chelating resin.

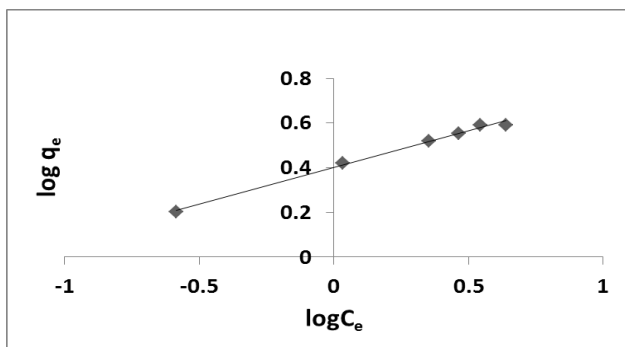


Fig (10): Freundlich adsorption isotherm of Ag^+ ions on (KNiHCF)-Ba-alginate at 25 °C.

The Temkin isotherm model is expressed by the following equation [24]:

$$q_e = B \ln K_T + B \ln C_e \tag{11}$$

where B and K_T are Temkin constants which represent the heat of adsorption & equilibrium binding constant, respectively. The values of B and K_T were obtained from the slope and intercept of linear plot of q_e versus $\ln C_e$ (Fig. 11) and shown in Table 1.

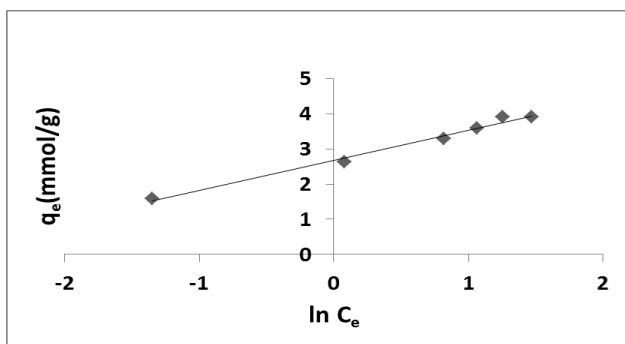


Fig (11): Temkin adsorption isotherm of Ag^+ ions on (KNiHCF)-Ba-alginate at 25 °C.

Table (1): The parameters of Langmuir, Freundlich and Temkin isotherms for (KNiHCF)-Ba-alginate at 25 °C.

Isotherms	Parameters	Ag^+
Langmuir	Q_{Max} (mmol/g)	3.064
	K (L/mmol)	0.632
	R^2	0.993
Freundlich	K_F (mmol/L)	2.511
	N	0.328
	R^2	0.995
Temkin	B	0.851
	K_T	23.22
	R^2	0.988

As shown in Table 1 the good fit experimental data with Langmuir, Freundlich, and Temkin isotherm models and high correlation coefficient (R^2) obtained for these plots indicated the validity of these models to Ba-alginate resin for Ag^+ ions. But Freundlich equation showed better results than Temkin and Langmuir models because of higher correlation coefficient for Ag^+ ions.

3. 2. 3. Effect of contact time on adsorption process

In order to determine the influence of contact time of (KNiHCF)-Ba-alginate in aqueous solution of Ag^+ ion at (pH 7, 25 °C and 7.41 mmol/L). Variations of adsorption capacity (q_e) versus time (20-180 min) were plotted, as shown in Fig.12. It was observed that the adsorption of Ag^+ ions from aqueous solution using the adsorbent was continuously increased with time increase until reaching equilibrium between two phases after 150 mins. Therefore, this obtained equilibrium time was selected for the next adsorption experiment.

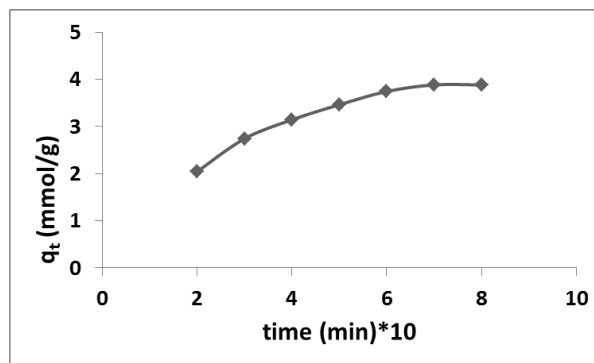


Fig (12): Effect of contact time of (KNiHCF)-Ba-alginate in aqueous solution of Ag^+ ion at (pH 7, 25 °C and 7.41 mmol/L).

The adsorption results were used to investigate the kinetic mechanism which controls the adsorption process. The most widely used models of Lagergren’s pseudo-first order; pseudo-second order and intra particle diffusion were used to investigate the kinetic process [25-27]. The linear form of the first order rate equation by Lagergren and Svenska [25] is expressed in Eq. 12:

$$\log (q - q_t) = \log q - \left(\frac{K_{ads}}{2.303} \right) t \tag{12}$$

where q_e and q_t are the adsorption capacity (mmol/g) at equilibrium and at time t (min), respectively. K_{ads} is the Lagergren rate constant (min^{-1}) of the adsorption. Plots of Eq.12 was made for Ag^+ ions sorption at different times and shown in Fig. 13. Lagergren constants were listed in Table.2.

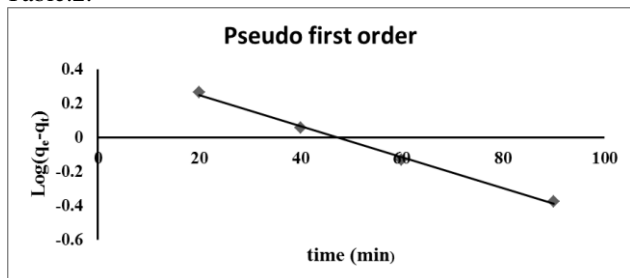


Fig (13): The first order kinetic plot of (KNiHCF)-Ba-alginate in aqueous solution of Ag^+ ion.

The experimental data were also treated according to pseudo-second model. The pseudo-second order model of Ho [26] can be expressed in the linearized form as follows:

$$\frac{t}{q_t} = \frac{1}{K_2 q^2} + \left(\frac{1}{q}\right) t \quad (13)$$

where K_2 ($\text{g mmol}^{-1} \text{min}^{-1}$) is the pseudo-second order rate constant. The kinetic plot of t/q_t versus t for Ag^+ ions sorption was presented in Fig. 14. The relationship was linear, and the value of the correlation coefficient (R^2) as shown in Table 2. The constants of the second order kinetic model plots were given in Table 2. Obviously, as it can be seen from the result listed in Table 2, correlation coefficient value (R^2) of the second order kinetic was higher than the value obtained from the first-order kinetics. Therefore, the sorption behavior Ag^+ ions onto (KNiHCF)-Ba-alginate obeys the second-order kinetics.

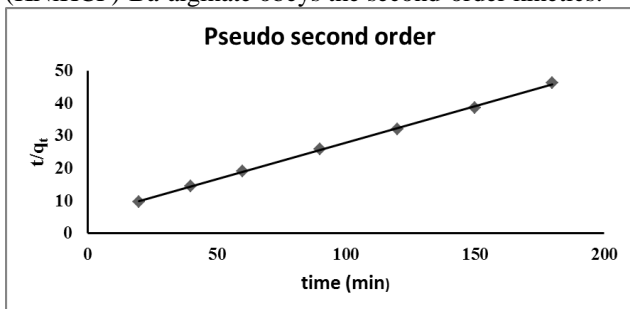


Fig (14): The second order kinetic plot of (KNiHCF)-Ba-alginate in aqueous solution of Ag^+ ion.

Intraparticle diffusion model is described using Eq. (14) proposed by Weber and Morris [27].

$$q_t = K_{id} t^{0.5} \quad (14)$$

where K_{id} is the intraparticle diffusion rate constant ($\text{mmol g}^{-1} \text{min}^{0.5}$). K_{id} was determined from the plot of q_t against $t^{0.5}$ (Fig.15). The constants of these plots are listed in Table 2. According to Weber and Morris, the adsorbate could be transported from the aqueous phase over adsorbent in three different steps as: (a) Diffusion of metal ions through the boundary layer to the surface of the chelating resin; (b) Intra-particle diffusion: migration of

metal ions from the outside surface of the chelating resin to the inside holes or pores of the resin through a pore diffusion or intra-particle diffusion mechanism; and (c) Adsorption of metal ions in an active area on the surface of chelating resin by the effect of chelation. With respect to Eq. (14), if the plot gives a straight line, intra-particle diffusion is accepted as the only rate-limiting step, but multi-linearity is formed which refers to two or more stages related to the adsorption of metal ions [28]. The adsorption process was restricted by three stages: (1) rapid transportation of metal ions from solution to the resin surface (2) gradual adsorption stage where intra-particle diffusion is rate-limiting step, and (3) final equilibrium stage where intra-particle diffusion begins to slow due to the very low metal ion concentration in the solution, in addition to fewer number of adsorption areas are available.

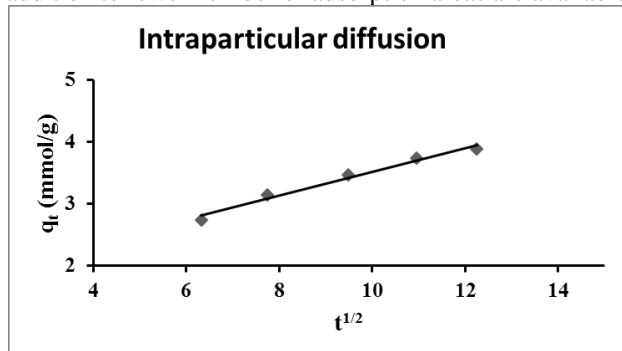


Fig (15): Weber-Morris intraparticle diffusion model of (KNiHCF)-Ba-alginate in aqueous solution of Ag^+ ion.

Based on these results, we can conclude that the intraparticle diffusion was not the only step of rate control. This behavior recommends that adsorption processes involve more than one single kinetic stage.

Table (2): Kinetic parameters for the adsorption of silver on (KNiHCF)- Ba-alginate.

Kinetic models	Parameters	Ag^+
Pseudo first order	K_1 (min^{-1})	0.021
	R^2	0.997
	$q_e(\text{theoretical})$ (mmol/g)	2.709
Pseudo second order	K_2 (g/ mmol m)	$9.23 \cdot 10^{-3}$
	R^2	0.999
	$q_e(\text{theoretical})(\text{mmol/g})$	4.454
	q_e (exp) (mmol/g)	3.884
Intraparticle diffusion model	K_{id} ($\text{mmol g}^{-1} \text{m}^{-0.5}$)	0.192
	R^2	0.981

3. 2. 4. Adsorption thermodynamics parameters

Thermodynamic parameters of the adsorption process were examined by performing the adsorption experiments at different temperatures (35, 45, 50 and 55 °C). Metal ion solution (100 ml, 7.41 mmol/L) equilibrated with 0.1 g of

Ba-alginate resin at optimum pH value. Equilibrium distribution coefficient (K_d) for the adsorption process was calculated by Eq. (15) [29].

$$K_d = \frac{(C_o - C_e)}{C_e} \times \left(\frac{V}{W}\right) \tag{15}$$

where C_o and C_e are the initial and equilibrium concentration of the metal ions in aqueous solution, respectively (mmol/L), V is the total volume of the solution (L) and W is the weight of the (KNiHCF)-Ba-alginate (g).

The standard enthalpy change (ΔH°_{ads}) and entropy change (ΔS°_{ads}) of the adsorption were estimated by plotting $\ln K_d$ versus $1/T$ according to Eq. (16) (Fig. 16).

$$\ln K_d = \frac{\Delta S^\circ_{ads}}{R} + \frac{\Delta H^\circ_{ads}}{RT} \tag{16}$$

where R is gas constant (8.314 J/mol K). The values of the slope and the intercept (Fig.16) give ΔH°_{ads} and ΔS°_{ads} , respectively.

Free energy change of the adsorption (ΔG°_{ads}) was calculated using the following equation:

$$\Delta G^\circ = -RT \ln K_d \tag{17}$$

Thermodynamic parameters involving ΔG°_{ads} , ΔH°_{ads} and ΔS°_{ads} for metal ion adsorption onto Ba-alginate resin were illustrated in Table 3. As it can be seen from Table 3, negative values of ΔH°_{ads} showed that the metal ion adsorption was an exothermic process [30, 31]. Also, the positive values of ΔS°_{ads} may be correlated with the increased randomness due to the liberation of H_2O of hydration during the adsorption of metal ions [32,33]. Finally, the thermodynamic parameters showed that there is continuity in adsorption process that is indicated by negative values of ΔG°_{ads} .

Table (3): Thermodynamic parameters for silver adsorption on (KNiHCF)-Ba-alginate.

ΔH° (kJ/mol)	-40.15
ΔS° (kJ/K mol)	+0.132
Temp. (K)	$-\Delta G^\circ$ (kJ/mol)
308	617.547
318	1521.18
323	2430.62
338	3288.9

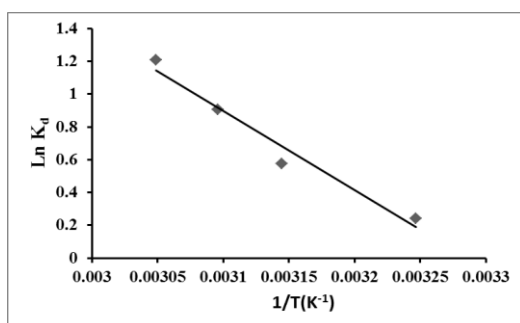


Fig (16): The effect of temperature on the distribution coefficient of Ag^+ ions onto (KNiHCF)-Ba-alginate.

3. 3. Uptake of metal ions using column technique

The break-through curves (C_{eff}/C_o vs. time) were obtained for Ag^+ sorption onto (KNiHCF)-Ba-alginate at different bed depth (9,18 cm), three constant influent flow rates (1,2,3 ml/min) at 0.41mmol/L single metal ion concentration. The mass transfer zone (Z_m), the sorption capacity of (KNiHCF)-Ba-alginate and removal percentage were calculated from the break-through curves by using equations 2-7 and presented in Table 4. According to results, (KNiHCF)-Ba-alginate showed a higher adsorption capacity for Ag^+ . The maximum sorption capacity was about for Ag^+ was about 1.146 mmol /g, respectively, at flow rate of 1 ml min^{-1} and bed height of 9 cm, which corresponds to 51.37 % for Ag^+ removal, respectively.

3.3.1. Effect of bed height

The break-through curves of sorption of Ag^+ was shown in Fig 7(a-c). As shown in Fig. 7, the shape of break-through curves of sorption of Ag^+ at both 1, 2 and 3 ml min^{-1} flow rates were significantly different as depth changed from 9 to 18cm. It was observed that the break-through time and exhaustion time were increased with increased in bed heights [32,33]. This may be due to the amount of resin was more to contact with Ag^+ ions. At higher bed heights a larger volume of metal solution could be treated as shown in Table 4 due to increase in the ratio of the resin where more active binding areas are available for processing the sorption process. The break-through time t_b , exhaustion time t_e , the height of mass transfer zone (Z_m) and percentage removal (R %) increased with rise in bed height. The increase in percentage removal must be related to the maximum saturation of all active sites in the adsorbent dosage by metal ions and broad ended mass transfer zone. The decreasing of uptake capacities by increasing the bed height is due to the change in volume to mass ratio [34,35].

3.3.2. Effect of flow rate

It was observed that the column performance is very well at lower flow rate. At higher flow rate, the break-through time and exhaustion time reached more rapid and this may be due to the inadequate residence time of the metal ion of Ag^+ with the resin [36]. The result reveals that the break-through curve becomes steeper as the flow rate increased. The metal sorption capacity decreases with increase in flow rate (Table4). This is because a much longer time is needed between the solute and that of the solid phase to reach equilibrium state. Therefore, this increase in flow rate causes a shorter presence time of the solute in the column and so, the metal ion leaves the column before equilibrium occurs [37]. Hence break-through time, bed exhaustion time, and sorption capacity were more at 1 ml min^{-1} when compared to 2, 3 ml min^{-1} flow rate.

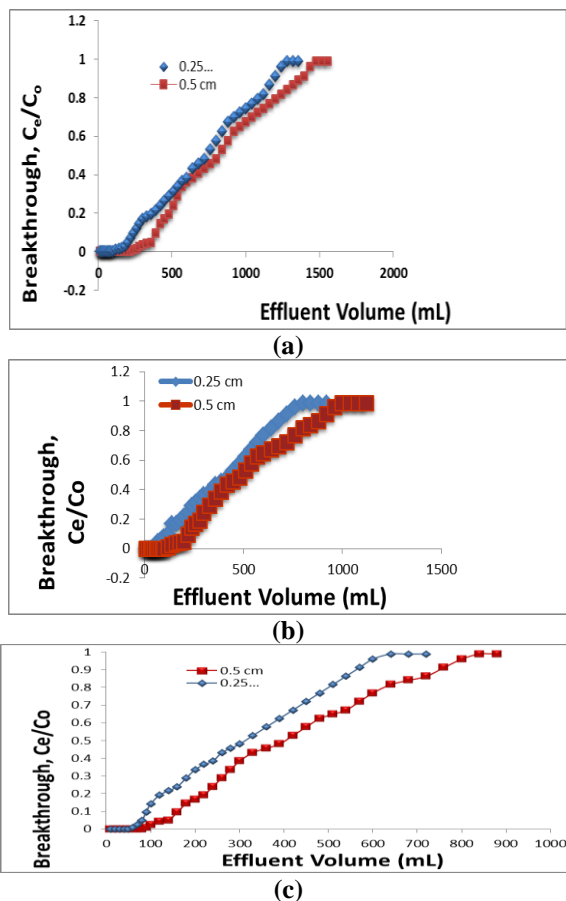


Fig (17): Break-through curves for (a) flow rate is 1 ml/min, (b) flow rate is 2 ml/min and (c) flow rate is 3 ml/min; initial concentration is 0.41 mmol/l, optimum pH and at 25 °C and bed depth (9, 18 cm).

3.3.3. Modeling of column experimental data

Various theoretical models such as Thomas and Yoon-Nelson models [38-40] were tested to show the experimental data related to the solute interaction behavior and to estimate the break-through curves.

3.3.3.1. Thomas model

The obtained data from the experiments were used to measure the adsorption capacity of (KNiHCF)-Ba-alginate and the adsorption rate constant using Thomas model based on Eq. (18).

$$\frac{C_{eff}}{C_o} = \frac{1}{1 + e^{\left[\frac{K_{Th} q_e m}{Q} - \frac{K_{Th} C_o V_{eff}}{Q} \right]}} \quad (18)$$

Where K_{Th} is the Thomas rate constant (l/mmol.min), m is the total dry weight of (KNiHCF)-Ba-alginate (g), V_{eff} is effluent volume, adsorption capacity of Ag^+ ion on

(mmol /g). The linearized form of Thomas model is given by Eq. (19).

$$\ln \left(\frac{C_o}{C_{eff}} - 1 \right) = \left[\frac{K_{Th} q_e m}{Q} - \frac{K_{Th} C_o V_{eff}}{Q} \right] \quad (19)$$

To detect maximum adsorption capacity of the adsorbent (q_e) and kinetic coefficient (K_{Th}) in Thomas model, experimental data were fit into the Eq. (19). This equation was used to fit the experimentally obtained data by plotting $\ln (C_o/C_{eff}-1)$ against the effluent volume. The Thomas rate constant and the ion exchange capacity were determined from the slope and intercept, respectively. The values of these two parameters are given in Table 4 for Ag^+ . According to Table 4 the calculated q_e from Thomas model is similar to the experimental q_e and the value of q_e decreased with increasing both flow rate and bed height. As can be observed, the experimental data are in good agreement with theoretical results.

3.3.3.2. Yoon Nelson model

The Yoon Nelson model expressed by Eq. (20) is based on the concept of the decrease in the adsorption for each adsorbate molecule is directly proportional to the probability of adsorbate breakthrough on the adsorbent.

$$\frac{C_{eff}}{C_o - C_{eff}} = e^{(K_{YN} t - \tau K_{YN})} \quad (20)$$

K_{YN} is the Yoon Nelson rate velocity constant (L/min), τ is the time in (min) required for 50 % adsorbate breakthrough. The linearized form of Yoon Nelson model is given by Eq. (21).

$$\ln \left(\frac{C_{eff}}{C_o - C_{eff}} \right) = \frac{K_{YN}}{Q} V_{eff} - \tau K_{YN} \quad (21)$$

To determine the rate constant (K_{YN}) and the time needed for 50 % adsorbate breakthrough, (τ) in Yoon Nelson model, experimental data were fit into the Eq. (21). This equation was used to fit the experimentally obtained data by plotting $\ln (C_{eff} / (C_o - C_{eff}))$ against the effluent volume. The Yoon Nelson rate constant and time required for 50 % adsorbate breakthrough (τ) were determined from the slope and intercept respectively. The values of two parameters are given in Table 4 for Ag^+ at 50 % breakthrough curve. The data in Table 4 also indicate that the τ value of model as similar to the τ_{exp} where τ_{exp} is the time required for Ag^+ 50 % adsorbate breakthrough from experiments in min. It was found that the time required for 50 % adsorbate breakthrough (τ) for increased with increasing bed height but decreased with increasing flow rate due to less residence time of metal ions in adsorbent bed. Since, the experimental data goes well with the model. Therefore, Yoon Nelson model is suitable model to describe fixed bed operations.

Table (4): Column data parameters, Thomas and Yoon Nelson Models constants at different flow rates and bed heights.

Variables			Calculated parameters				Thomas model				Yoon Nelson model			
Metal ion	Q (mL/min)	Z (cm)	q _{total} (mmol)	q _e (mmol/g)	t _b (min)	t _e (min)	Δt (min)	R %	Z _m (cm)	q _e (mmol/g)	K _{th} (mL/mmol.min)	R ²	K _{YN} (min ⁻¹)	T min
Ag(I)	1	9	0.286	1.146	100	1200	1100	51.37	8.3	1.161	9.756	0.997	0.004	707.675
	1	18	0.332	0.664	220	1480	1260	51.91	15.3	0.636	8.54	0.996	0.0035	775.143
	2	9	0.327	1.306	40	800	760	86.57	8.2	0.675	27.80	0.989	0.0114	205.63
	2	18	0.206	0.412	100	1000	900	44.88	16.2	0.395	23.41	0.992	0.0096	241.05
	3	9	0.124	0.496	50	640	590	42.03	8.3	0.499	53.4	0.995	0.0219	101.40
	3	18	0.155	0.309	70	800	730	42.91	16.4	0.297	45.37	0.992	0.0186	120.83

4. Conclusion

Spherical beads have been prepared by ionotropic gelation of nickel chloride, potassium ferrocyanide with sodium alginate in the presence of BaCl₂ solution. The composition, properties and morphology of the resulting resin have been characterized by Fourier transform infrared (FTIR) spectroscopy, scanning electron microscopy (SEM), thermo gravimetric analysis (TGA) and x-ray. This resin have high sorption capacity for Ag⁺ from its aqueous medium. The sorption of metal ion onto (KNiHCF)-Ba-alginate was influenced by several factors such as the solution pH, concentration of metal ions, contact time and solution temperature. In batch equilibrium adsorption method, the optimum sorption pH

for Ag⁺ was 7. The adsorption process followed the Freundlich isotherm model indicated that the heterogeneous sorption is dominant. The kinetic experiments showed that adsorption well fits to pseudo-second order model. Thermodynamic parameters suggest that adsorption of metal ion on (KNiHCF)-Ba-alginate was spontaneous and exothermic in nature. (KNiHCF)-Ba-alginate was efficient for Ag⁺ removal by batch but also by column methods, and the best condition for adsorption process at 1ml/min and 9 cm bed height. Thomas and Yoon Nelson models are suitable models to describe fixed bed column operations.

References

- [1] A. Heidari, H. Younesi, Z. Mehrabanb, Chem. Eng. J., 153 (2009) 70–79.
- [2] J. P. Chen, L. Wang, Chemosphere, 54 (2004) 397–404
- [3] K.N. Ghimire, H. Kai, K. Inoue, K. Ohto, H. Kawakita, H. Harada, M. Morita, Bioresource Technology, 99 (2008) 2436-2441.
- [4] H.Aydn, Y. Bulut, C. Yerlikaya, Journal of Environmental Management, 87 (2008) 37-45.
- [5] E. S. Z. El-Ashtouky, N. K. Amin, O. Abdelwahab, Desalination, 223 (2008) 162-173.
- [6] C. Chen, and J. Wang, J. Hazard. Mater, 151 (2008) 65-70.
- [7] A. K. Meena, K. Kadirvelu, G. K. Mishra, C. Rajagopal, P. N. Nagar, J. Hazard. Mater, 150 (2008) 604-611.
- [8] A. Kapoor, T. Viraraghavan, D. R. Cullimore, Bioresour. Technol., 70 (1999) 95-104.
- [9] R. Amils R. and Ballester A. (Ed.) biohydrometallurgy and the environment toward the mining of the 21st century, vol. 1, Elsevier, chapter (1) (1999) 143–152.
- [10] M. A. Barakat, Arab. J. Chem. 4 (2011) 361–377.
- [11] G. Dermont; M. Bergeron; G. Mercier; M. Richer-Lafleche, Practice Periodical of Hazardous, Toxic, and Radioactive Waste Management, 12 (2008) 188-209.
- [12] S. A. Khan, R. Rehman, M. A. Khan Waste Manag., 15 (1995) 271–282.
- [13] P. Hanzlík, J. Jehlička, Z. Weishauptová, O. Šebek, plant soil environ. , 50 (2004) 257–264
- [14] J. Ho, Y. Ning, H. Wang, S. Khoo, Y. Chen, C. Chow, 20(2014) 337-343.
- [15] U. Rakchaiyawan, Y. Kulratkitiwong, K. Piyamongkala, IJESD, 6 (2015) 655-659.
- [16] D. F. Lawler, A. M. Mikelonis, I. Kim, B. L. Lau, S. Youn, Water Science & Technology: Water Supply, 13 (2013) 1181-1187.
- [17] A. Gedanken, E. Givataim, E. Tel-Or, K. Bilu, B. Chefetz, K.smadar Elmesal US 2010/0218645 A1, 2010.
- [18] H. Kalavathy, B. Karthik, L.R. Miranda, Colloids Surf. B., 78 (2010) 291-302.
- [19] C. M. Futralan, C. C. Kan, M. L. Dalida, C. Pascua, M.W. Wan, Carbohydr. Polym., 83 (2011) 697-704.
- [20] I. Langmuir, J. Am. Chem. Soc., 40(1918) 1361–1403.
- [21] T. W. Weber, R. K. Chakravot, AIChE J., 20 (1974) 228–238.
- [22] A. Sari, M. Tuzen, D. Citak, M. Soylak, J. Hazard. Mater., 149 (2007) 283–291.
- [23] X. S. Wang, J. Huang, H. Q. Hua, J. Wang, Y. Qin, J. Hazard. Mater., 142 (2007) 468–476.
- [24] H. Freundlich, Phys. Chem. Soc., 40 (1906) 1361–368.

- [25] M.J. Temkin, V. Phyzev, U.S.S.R., 12 (1940) 217–222.
- [26] Y. S. Ho, *Scientometrics*, 59 (2004) 171–177.
- [27] Y. S. Ho, *J. Hazard. Mater.*, 136 (2006) 681–689.
- [28] W. J. Weber, J. C. Morris, *J. Sanitary Eng. Div.*, 90 (1964) 79–108.
- [29] C. Sarici-Ozdemir, Y. Onal, *Desalination*, 251(2010) 146–152.
- [30] A. Nilchi, R. Saberi, M. Moradi, H. Azizpour, R. Zarghami, *Chem. Eng. J.*, 172 (2011)572–580.
- [31] S. M. El-Bahy, Z. M. El-Bahy, *Korean J. Chem. Eng.*, 33 (2016) 2492–2501.
- [32] S. M. El-Bahy, Z. M. El-Bahy, *J. Environ. Chem. Eng.* 4 (2016) 276–286.
- [33] M. C. Fournier-Salaun, P. Salaun, *Cent. Eur. J. Chem.*, 5 (2007)1083-1093.
- [34] N. Yahaya, I. Abustan, M. Latiff, O. Solomon Bello, M. A. Ahmad, *Inter. J. Eng. Technol.*, 11(2011) 248-252
- [35] A. Shahbazi, H. Younesi, A. Badiei, *Can. J. Chem. Eng.*, 91 (2013) 739–750.
- [36] S. Singha, U. Sarkar, S. Mondal, *Desalination*, 297 (2012) 48-58.
- [37] O. Hamdaoui, *J. Hazard. Mater.*, 138 (2006) 293-303.
- [38] R. Han, D. Ding, Y. Xu, W. Zou, Y. Wang, Y. Li, L. Zou, *Bioresour. Technol.*, 99 (2008) 2938-2946.
- [39] R. Han, Yu. Wang, X. Zhao, Y. Wang, F. Xie, J. Cheng, M. Tang, *Desalination*, 245 (2009) 284-297.
- [40] M. Calero, F. Hernáinz, G. Blázquez, G. Tenorio, M.A. Martín-Lara, *J. Hazard. Mater.*, 171 (2009) 886-893.